SEMARAK ILMU PUBLISHING

Journal of Advanced Research in Applied Mechanics

Journal homepage:
https://semarakilmu.com.my/journals/index.php/appl_mech/index
ISSN: 2289-7895

Evaluation of Graphite Size of Modified Ductile Ni-Resist with Higher Manganese

Khairul Ihsan Yaakob[1], Mohd Rashidi Maarof[1,2,*], Muhammad Aminuddin Rosnizan[1], Mohamed Reza Zalani[1], Asnul Hadi Ahmad[1]

[1] Manufacturing Research Focus Group (MFG), Faculty of Mechanical and Automotive Engineering Technology, Universiti Malaysia Pahang (UMP), 26600 Pekan, Pahang, Malaysia
[2] Automotive Engineering Centre, Universiti Malaysia Pahang (UMP), 26600 Pekan, Pahang, Malaysia

ARTICLE INFO

Article history:
Received 28 October 2024
Received in revised form 29 November 2024
Accepted 6 December 2024
Available online 30 December 2024

Keywords:
Metal casting; oxidation; Ni-Resist

ABSTRACT

These days, batteries, applications requiring high temperatures, and corrosive environments are the main uses for nickel. The rise in electric and hybrid vehicles has increased the amount of nickel used as the primary component in alloys. Because of this, the price of nickel had peaked and was now fluctuating to attract manufacturers. One compound that is impacted is the Ni-Resist alloy. In this work, the nickel weight percentage of an alloy known as ductile Ni-resist alloy was reduced in order to reduce processing costs. The modification was looked into in an effort to minimize the cost of the alloying process by using less nickel in the alloying composition. The modification was looked into in an effort to minimize the cost of the alloying process by using less nickel in the alloying composition. During the melting stage, 10 weight percent nickel was added along with up to 12 weight percent chromium and manganese. Next, the impact of the alloying elements was investigated with respect to its mechanical characteristics and microstructure behavior. Then the graphite formation after alloy solidification was characterize to evaluate its dimension size.

1. Introduction

In order to become more competitive, manufacturers have developed commercial vehicles more quickly (comparative to product life cycle) over the past few decades. In order to stay competitive, extensive research was conducted on new alloy types to guarantee their sustainability or to investigate better alloys to guarantee the component can be sustained in harsh and demanding environments. The recent research has affected certain alloys, including Ni-Resist alloy, which is used for dynamic load at elevated temperatures. The sub-category of Ductile Ni-Resist (DNR) alloy includes the austenite structure of the graphite nodules that make up the Ni-Resist alloy. Because of its high strength-to-weight ratio, good machinability, and generally good mechanical properties at elevated temperatures, this material was developed for high temperature applications. It also has an

* *Corresponding author.*
E-mail address: mrashidi@umpsa.edu.my

https://doi.org/10.37934/aram.130.1.130139

austenitic matrix at all temperatures. In contrast, cast iron and steel experience a critical range in applications where temperatures can reach up to 675^{o}C, which frequently causes castings to fracture and distort.

Volume changes, which result from matrix phase shifts between ferrite and austenite, cause this phenomenon. DNR alloys contribute to high temperature applications because they have an austenitic matrix at all temperatures and do not undergo this transformation. It is accomplished during the material casting process by appropriately alloying base iron. The Time-Temperature-Transformation (T-T-T) curve is typically shifted to the right with the appropriate addition of alloying elements, allowing one to avoid the T-T-T curve's "nose" [1]. At room temperature, an austenite microstructure can form and hold. Heat treatment is not used in this process. Because of these remarkable qualities, DNR can be used instead of austenitic steel in oil, gas, automotive, and power plant applications [2].

According to a recent study, nickel (Ni) is a successful primary alloying element for the processing of DNR alloy. Ni, which is present in the metal composition and functions as an austenite matrix stabilizer, has an influence on the process and causes the DNR alloy's as-cast austenite microstructure to emerge. At least 18 weight percent, Ni suppresses the austenite (γ) → ferrite (α) transition into conventional ductile iron [3]. Even though nickel is successful in changing the iron phase into an austenite structure, its use is not inexpensive. Ni is known to be a relatively costly raw material, and alloying DNR alloy is economically constrained by its high cost. So, there are studies were conducted to lower the Ni/wt% in an effort to minimize production costs. Thirteen weight percent was the least amount of Ni/wt% that was effectively used to convert alloyed iron to austenite structure [4]. The potential of manganese (Mn) and copper as a substitute for the DNR alloying element has been documented in another study. The outcome of the experiment, however, indicated a negative impact. Morrison [3] suggests that although copper can form an austenite structure, the process has a negative effect on the DNR alloy's nodule graphite. The nodule's shape was altered while it solidified. On the other hand, Mn, a different candidate, simultaneously promotes the formation of carbides and stabilizes austenite. Morrison also stated that an alloy can be categorized as free carbide DNR alloy if it contains less than 4 weight percent Mn.

As was previously discussed, adding more manganese to the mixture will not cause free graphite to solidify directly into nodule graphite. Rather, it promotes the formation of carbide. To reduce the production of carbide, an inoculation technique is used as a remedy. According to reports, inoculation can significantly enhance the distribution and graphite form of conventional ductile iron, as suggested by Jincheng [5]. Furthermore, Choi *et al.,* [6] report that inoculation enhances the undercooling effect during the casting solidification of conventional cast iron. Similarly, he proposed that for conventional ductile iron, inoculation can generally enhance the graphite form and distribution. Inoculation is suggested as a possible remedy in their investigation to enhance the undercooling effect during casting solidification. Jiyang [7] found that by refining the material structure, the cooling curve may affect the solidification process as a whole. The modification can be accomplished by inoculation, which reorganizes the distribution of the graphite structure rather than the carbide distribution. The method allows solidification cooling curves to be used to monitor the undercooling phenomenon. Consequently, the region that solidifies last and the segregation factor are reduced. On the other hand, no studies about how the inoculation procedure affected the modified DNR alloy with a higher manganese weight percentage have been released.

The literature on corrosion of DNR austenitic matrix alloy is generally limited because most researchers focused more on austenitic steel than austenitic iron. An intriguing subject is the Austenitic region, whether it is for iron or steel. Components of exhaust systems, boilers, and turbochargers are examples of applications where the austenitic zone occurs and is stable at high

temperatures. Because of this, researchers are eager to bring the austenitic zone to any temperature—both room temperature and high—by alloying steel or iron with a precise composition. So, when the Fe-Mn-Al-Si alloy's composition and scale morphology were examined by Anderson and Vanessa [8] they discovered oxidation resistance has been found to occur between 600 and 900 ^{o}C. The moderate oxidation resistance is caused by the presence of an additional phase (oxides of Al, Mn, and Fe) following the oxidation. Tjong [9] investigated the possibility of producing FeAlMnC by substituting Mn for Cr and Ni. He observed mechanical properties that are feasible at cryogenic temperatures in his research. The microstructure and mechanical characteristics of modified DNR alloy with a higher manganese content were investigated by Rashidi and Hasbullah [10]. The oxidation test was not performed, though. Heat-resistant Si-Mo ductile cast iron's mechanical characteristics and oxidation resistance were examined by Kim *et al.,* [11]. The outcomes demonstrated that the alloy can be improved by changing individual alloy elements.

This study aims to combine both Ni and Mn at a specific composition to produce similarity of modified DNR alloy. Mn/wt% rises to as high as 12 wt%, while Ni/wt% decreases to as low as 10 wt%. The altered alloy's microstructure ought to contain a graphite nodule and form an austenite structure. Then this study attempts to investigate the impact of high manganese weight percentage alloy on the nodular graphite formation of modified DNR alloy. The goal is to understand how the modified DNR alloy's graphite behavior relates to the casting's microstructural inhomogeneity. The application of DNR alloy exposes components to a moderately high temperature, which is why the emphasis is considered significant.

2. Methodology

The current investigation was carried out in an induction furnace with a 50 kg holding capacity, 200 kW of power, and a 1000–3000 Hz frequency range. To create modified DNR alloy with the desired composition, the following charge materials (steel scrap, pig iron, and pure nickel) were used: (a) 9Mn-10Ni; (b) 10Mn-10Ni; (c) 11Mn-10Ni; and (d) 12Mn-10Ni wt%. Ferro-Manganese (FeMn) and Ferro-Chrome (FeCr) were added after stirring sessions to raise the content of manganese and chromium, as shown by Rashidi and Hasbullah [10]. Before being poured into a mold at 1400+20^{o}C, the melt was cleaned and superheated to 1500+20^{o}C. To create a green sand mold, a combination of silica sand, bentonite, and water was used to make the mold. Both the inoculation and the magnesium treatment were carried out using the in-mould method. In the mold reaction chamber, 1.1 weight percent nodularizer was added using FeSiMg, which has a 5% magnesium content and a sizing of roughly 1-4 mm [10]. Once the nodulant was found, the inoculant was added to the mold reaction chamber at a weight percentage of 0.5, as shown in Figure 1. The chemical compositions of all types of experimental iron, nickel, FeMn, FeCr, nodularizer, and inoculant are listed in Table 1. Each casting's runner system has a properly constructed chamber where the inoculant and nodulant were inserted. The reaction chamber's design and the in-gate's placement were separated by 120 mm. To prevent fading and promote inoculant dissolution, a grading-size inoculant of 0.2 to 0.7 mm was used. To obtain microstructural specimens, test specimens from ASTM A439 Y-blocks were sectioned, grounded, and polished using 0.3 µm alumina powder. A second set of sample coupons was cut to measure 15.0 x 15.0 x 2.0 mm. They were subsequently polished with 1.0 µm diamond paste after being mechanically ground to 2400 mesh on SiC paper. Following a mirror-finish polish, the samples were cleaned using ultrasonic agitation for 10 minutes in ethanol and then acetone. Before being exposed, the samples were dried and kept in a desiccator. X-ray energy dispersive spectroscopy (EDS) was used to analyze the specimens' chemical compositions after a scanning electron microscope (SEM) was used to characterize the scales that had formed on their surface. On

a few fractured specimens, a copper-plated was applied to safeguard the scales while a cross-sectional metallographic view was being prepared. The EDS model Philips XL40 system was used to perform the chemical analysis.

Fig. 1. Experimental setup during molten metal pouring

Table 1
Chemical composition of iron, alloyed materials, nodularizer, inoculant, FeMn and FeCr (wt %)

	Element										
	C	Si	Mn	P	S	Mg	Ni	Ca	Cr	R.E	Fe
Pig iron	2.91	2.28	0.12	0.07	0.02	-	0.02	-	-	-	Balance
Steel	0.20	0.15	0.60	0.03	0.02	-	-	-	-	-	Balance
Nickel	-	-	-	-	-	-	99.00	-	-	-	Balance
FeMn	-	1.00	86.00	0.10	0.02	-	-	-	-	-	-
FeCr	8.00	4.00	-	0.04	0.04	-	-	-	60.0	-	-
Nodularizer	-	44.00	-	-	-	5.00	-	2.00	-	1.90	-
Inoculant	-	70.00	-	-	-	-	-	2.00	-	-	Balance

3. Results

3.1 Microstructure Evaluation

A hypoeutectic composition alloy containing different component alloys containing Fe, C, Si, Mn, Ni, and other constituents was produced during the casting process. Solidification involved a number of processes, including phase formation, element solubility, and segregation, to mention a few. Subsequent analysis reveals that this alloyed iron is composed of multiple phases, including carbides, graphite aggregate, eutectic austenite, austenite matrix, and impurity inclusion [12] and [13]. The graphite forms of all specimens don't appear to be full nodular. Furthermore, a flake graphite microstructure was discovered, which affected the percentage of the overall nodule graphite shape.

These results show that austenitic ductile iron's graphite was less spherical than that of common ductile iron (Figure 2).

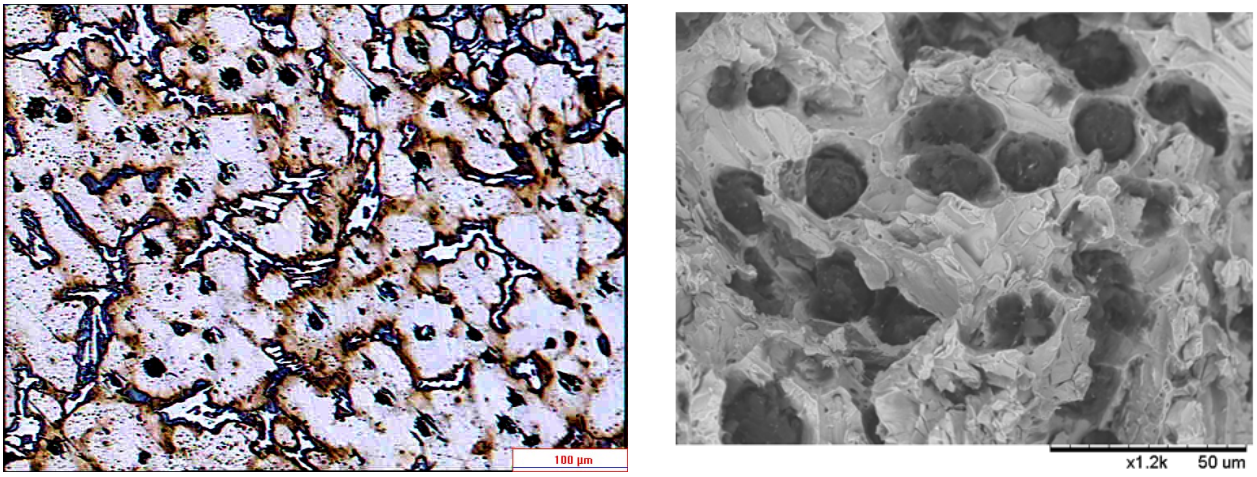

(a) (b)

Fig. 2. Distribution of nodule graphite shape in alloyed iron (a) by microscope and (b) by SEM application

The parameter size of the nodule was categorized as follows: 1 to 10 µm, 10 to 20 µm, and so forth. For 8% manganese, Figure 3(a) indicates that most nodule sizes fall between 1 and 10 µm. It attains 20.9–36.0% of the total size. 10.3–30 µm nodule graphite size accounts for 13.3–32.2% of the total nodule size. The quantity decreases to a size of 30 to 40 µm, or 6.0 to 19.4% of the total size. One rarely finds such a nodule in sizes greater than 40 µm. Lower inoculation results in smaller nodule graphite size (below 20 µm) in the interim. However, a wider percentage of nodule area size up to 40 µm is generated by higher inoculation. The sizes were closely spaced.

As illustrated in Figure 3(b), at 10% manganese, inoculation does affect the formation of nodule graphite at greater uniformity, with 40.1 to 69.9% of total nodule sizing in the range of 1 to 10 µm. The trend quickly decreases to a size of 10 to 20 µm, with 12.8 to 29.9% of nodules in this range. At a nodule size of 20 to 30 m, the percentage decreases even more, from 4.5 to 11.4%. The quantity is much less than 5.0% after that.

Figure 3(c) illustrates that at 11% manganese, the percentage of nodule size is typically between 1 and 20 µm. It attains 15.2 to 38.1 percent of the total size. A nodule larger than 20 µm typically yields a reading of less than 10.0%. Rarely do nodules larger than 30 µm exist. Although the nodule size distribution was not widely distributed, the nodule size trend decreased in line with the preceding manganese percentage.

The inoculation influences the formation of nodule graphite at greater uniformity when 34.5 to 41.8% of the total nodule sizing 1 to 10 µm, as shown in Figure 3(d) at 11% manganese. Of the total nodules, 30.9 to 32.0% have sizes between 10 and 20 µm. The trend quickly decreases to a size of 20 to 30 µm, with 9.1 to 13.8% of nodules in that range. Subsequently, the amount falls significantly below 6.7%. These results demonstrate that nodule size below 30 µm was consistently influenced by inoculation. A smaller nodule size could also be a reflection of late-stage graphite formation during solidification. In summary the graphite is well distributed alongside modified DNR with almost spherical shape (Figure 4)

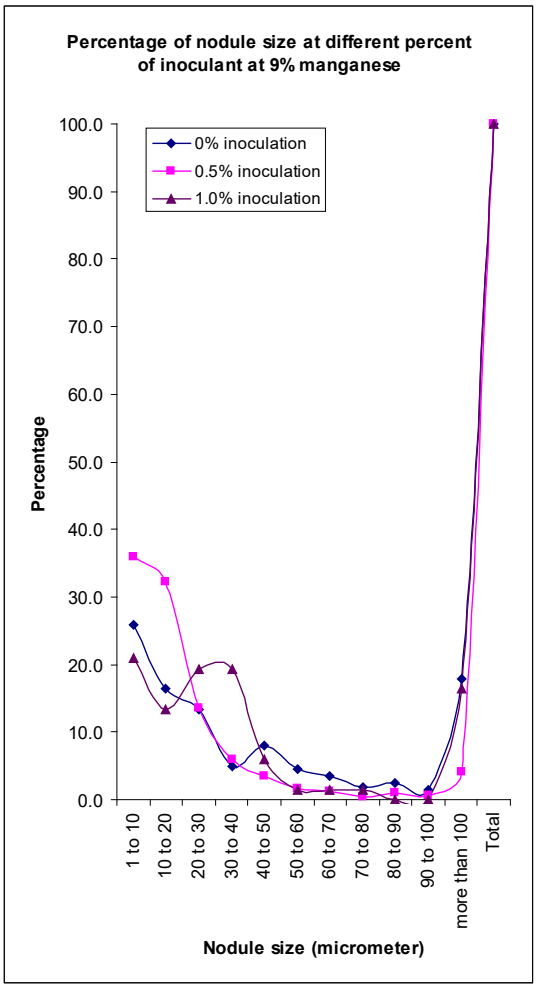
Percentage of nodule size at different percent of inoculant at 9% manganese
0% inoculation
0.5% inoculation
1.0% inoculation
Percentage
100.0
90.0
80.0
70.0
60.0
50.0
40.0
30.0
20.0
10.0
0.0
1 to 10
10 to 20
20 to 30
30 to 40
40 to 50
50 to 60
60 to 70
70 to 80
80 to 90
90 to 100
more than 100
Total
Nodule size (micrometer)

(a)

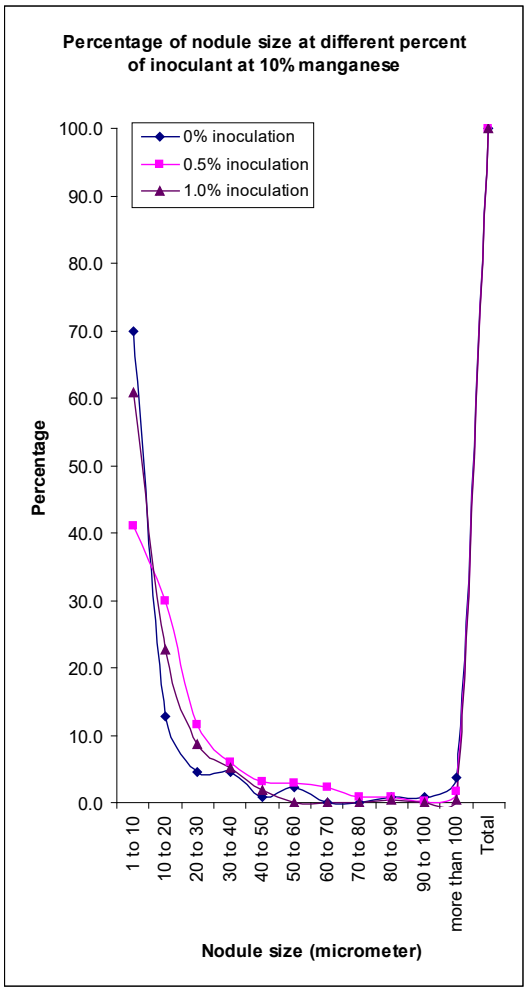
Percentage of nodule size at different percent of inoculant at 10% manganese
0% inoculation
0.5% inoculation
1.0% inoculation
Percentage
100.0
90.0
80.0
70.0
60.0
50.0
40.0
30.0
20.0
10.0
0.0
1 to 10
10 to 20
20 to 30
30 to 40
40 to 50
50 to 60
60 to 70
70 to 80
80 to 90
90 to 100
more than 100
Total
Nodule size (micrometer)

(b)

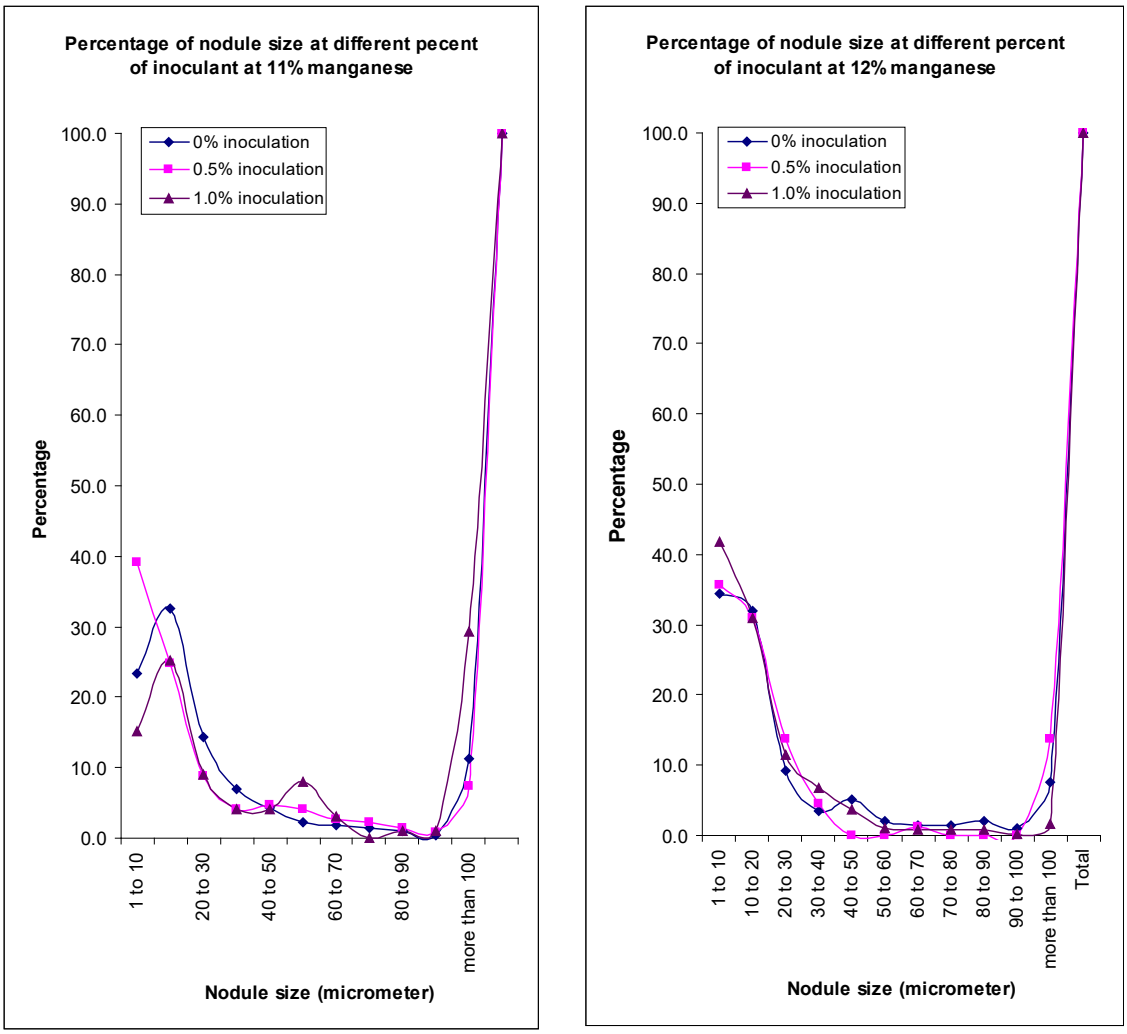

(c) (d)

Fig. 3. Percentage of graphite nodule size at different inoculants percentage (a) 9 %, (b) 10 %, (c) 11 % and (d) 12 % manganese consumption respectively

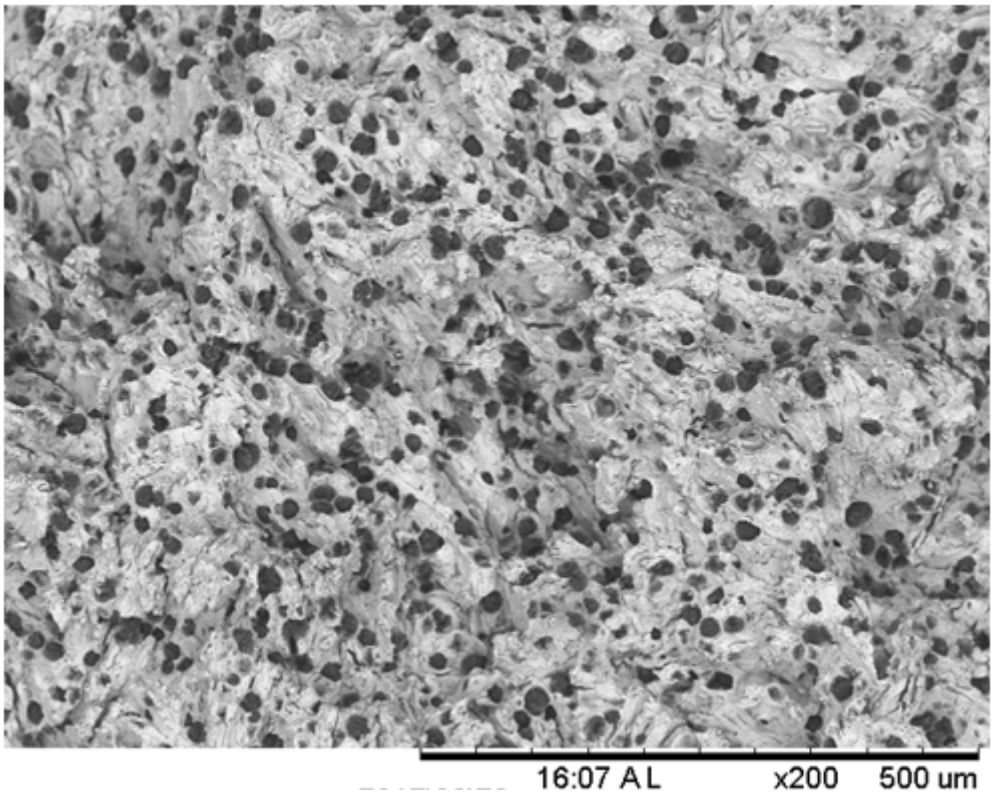

(a)

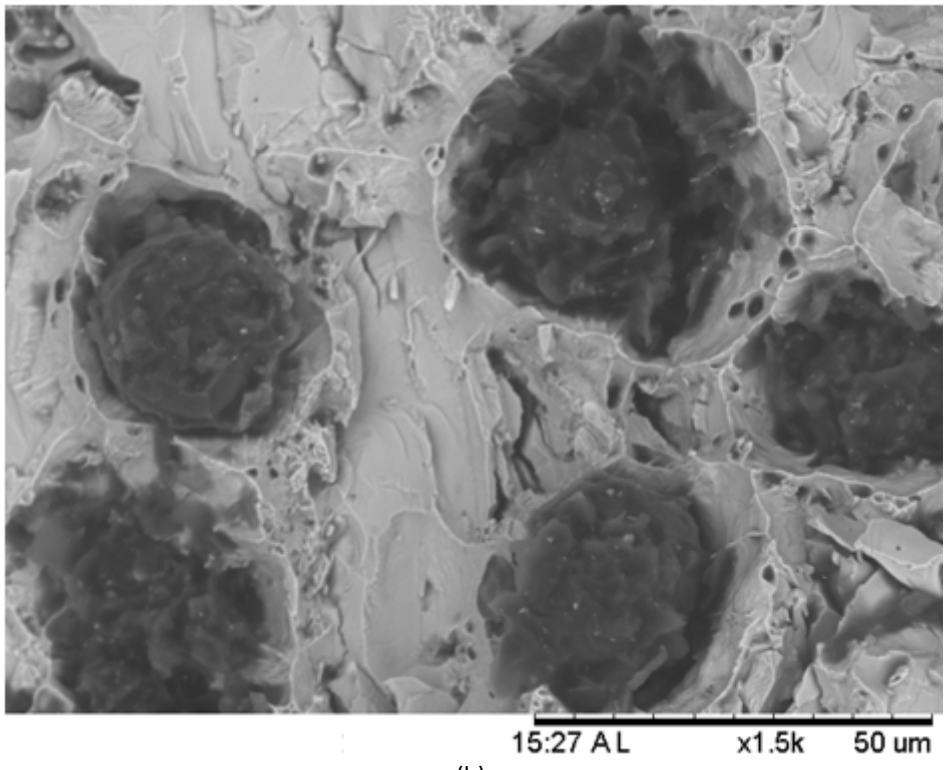

(b)

Fig. 4. Micrograph show distribution of nodule graphite (a) and mixed shape of nodular graphite shape

It's possible that the nodularity condition reflects the solidification path. The formation of austenite dendrites marks the beginning of the recognized solidification path. Austenite and graphite then grow as distinct eutectic materials [14] and [15]. Liquid metal formed spheroidal graphite, which

was then encased in austenite. Austenite affects the roundness of graphite. However, that was limited to specimens that were quickly cooled or quenched, which stopped carbon from diffusing from liquid to graphite [16] and [17]. In order to facilitate carbon atom diffusion along the liquid channels separating the austenite grains, this study used slow cooling. Nodule graphite grows inhomogeneously as a result. Furthermore, impacted is the nodularity.

4. Conclusions

This paper describes the formation of a mixture of graphite nodule sizes and dimensions (full nodule, halves and lesser) in an alloyed iron. The nodule's formation from magnesium treatment shortly before solidification sets it apart from the untreated flake graphite shape. Those nodules, while having a nearly identical pattern, vary in size at different manganese additions. The majority of the dimensions showed up as 10–30 micron sizes. Because of the potential for being trapped in the grain structure at an earlier stage of development, the graphite cannot grow to a larger size. Along the grain boundary, investigation also reveals a Late to Freeze region.

Acknowledgement

This research was funded by a grant from Ministry of Higher Education of Malaysia (FRGS Grant FRGS/1/2022/TK10/UMP/02/64 - RDU220135) and university's internal grant (RDU220305).

References

[1] Çelik, Gülşah Aktaş, Maria-Ioanna T. Tzini, Şeyda Polat, Ş. Hakan Atapek, and Gregory N. Haidemenopoulos. "Thermal and microstructural characterization of a novel ductile cast iron modified by aluminum addition." *International Journal of Minerals, Metallurgy and Materials* 27 (2020): 190-199. https://doi.org/10.1007/s12613-019-1876-8

[2] Xiang, Shengmei, Stefan Jonsson, Baohua Zhu, and Joakim Odqvist. "Corrosion fatigue of austenitic cast iron Ni-Resist D5S and austenitic cast steel HK30 in argon and synthetic diesel exhaust at 800° C." *International Journal of Fatigue* 132 (2020): 105396. https://doi.org/10.1016/j.ijfatigue.2019.105396

[3] Morrison, J. C. "Corrosion behaviour of Ni-Resist cast irons." *Anti-Corrosion Methods and Materials* 30, no. 8 (1983): 8-9. https://doi.org/10.1108/eb007227

[4] Fatahalla, Nabil, Aly AbuElEzz, and Moenes Semeida. "C, Si and Ni as alloying elements to vary carbon equivalent of austenitic ductile cast iron: Microstructure and mechanical properties." *Materials Science and Engineering: A* 504, no. 1-2 (2009): 81-89. https://doi.org/10.1016/j.msea.2008.10.019

[5] Jincheng, Xu. "Ecodesign for wear resistant ductile cast iron with medium manganese content." *Materials & Design* 24, no. 1 (2003): 63-68. https://doi.org/10.1016/S0261-3069(02)00076-6

[6] Choi, J. O., J. Y. Kim, C. O. Choi, J. K. Kim, and P. K. Rohatgi. "Effect of rare earth element on microstructure formation and mechanical properties of thin wall ductile iron castings." *Materials Science and Engineering: A* 383, no. 2 (2004): 323-333. https://doi.org/10.1016/j.msea.2004.04.060

[7] Jiyang, Zhou. "Colour metallography of cast iron." *China foundry* 6, no. 1 (2009): 57-69.

[8] Dias, Anderson, and Vanessa de Freitas Cunha Lins. "Scale morphologies and compositions of an iron-manganese-aluminum-silicon alloy oxidated at high temperatures." *Corrosion science* 40, no. 2-3 (1998): 271-280. https://doi.org/10.1016/S0010-938X(97)00134-0

[9] Tjong, S. C. "Electron microscope observations of phase decompositions in an austenitic Fe-8.7 Al-29.7 Mn-1.04 C alloy." *Materials Characterization* 24, no. 3 (1990): 275-292. https://doi.org/10.1016/1044-5803(90)90055-O

[10] Rashidi, Maarof Mohd, and Mohd Hasbullah Idris. "Microstructure and mechanical properties of modified ductile Ni-resist with higher manganese content." *Materials Science and Engineering: A* 574 (2013): 226-234. https://doi.org/10.1016/j.msea.2013.02.038

[11] Kim, Yoon-Jun, Ho Jang, and Yong-Jun Oh. "High-temperature low-cycle fatigue property of heat-resistant ductile-cast irons." *Metallurgical and Materials Transactions A* 40 (2009): 2087-2097. https://doi.org/10.1007/s11661-009-9911-4

[12] Stan, Iuliana, Denisa-Elena Anca, Iulian Riposan, and Stelian Stan. "Solidification pattern of 4.5% Si ductile iron in metal mould versus sand mould castings." *Journal of Thermal Analysis and Calorimetry* 148, no. 5 (2023): 1805-1817. https://doi.org/10.1007/s10973-022-11832-4

[13] Mrvar, Primož, Mitja Petrič, and Milan Terčelj. "Thermal Fatigue of Spheroidal Graphite Cast Iron." In *TMS Annual Meeting & Exhibition*, pp. 406-415. Cham: Springer Nature Switzerland, 2023. https://doi.org/10.1007/978-3-031-22524-6_37

[14] Sangame, Bahubali Babanrao, Y. Prasannatha Reddy, and Vasudev D. Shinde. "Analyzing the effect of inoculant addition on the solidification of ductile cast irons using thermal analysis." *World Journal of Engineering* ahead-of-print (2022). https://doi.org/10.1108/WJE-07-2022-0272

[15] Bauer, Branko, Ivana Mihalic Pokopec, Mitja Petrič, and Primož Mrvar. "Effect of bismuth on preventing chunky graphite in high-silicon ductile iron castings." *International Journal of Metalcasting* 14 (2020): 1052-1062. https://doi.org/10.1007/s40962-020-00419-0

[16] Liu, Jin-hai, Jian-shuai Yan, Xue-bo Zhao, Bin-guo Fu, Hai-tao Xue, Gui-xian Zhang, and Peng-hui Yang. "Precipitation and evolution of nodular graphite during solidification process of ductile iron." *China Foundry* 17 (2020): 260-271. https://doi.org/10.1007/s41230-020-0042-2

[17] Chatcharit, Kiattisaksri, Akira Sugiyama, Kohei Morishita, Taka Narumi, Kentaro Kajiwara, and Hideyuki Yasuda. "Time evolution of solidification structure in ductile cast iron with hypereutectic compositions." *International Journal of Metalcasting* 14 (2020): 794-801. https://doi.org/10.1007/s40962-020-00424-3